Progress In Electromagnetics Research Letters, Vol. 21, 79–88, 2011

EXPERIMENTAL OBSERVATION OF PULSE-SHORTENING PHENOMENA IN TRAVELING-WAVE FIELD EFFECT TRANSISTORS

K. Narahara

Graduate School of Science and Engineering
Yamagata University
4-3-16 Jonan, Yonezawa, Yamagata 992-8510, Japan

Abstract—We experimentally characterize the pulse-shortening phenomena in traveling-wave field effect transistors (TWFETs). When a decreasing voltage pulse is applied to the gate line and an increasing voltage pulse is simultaneously applied to the drain line, a sinusoidal wave supported by an exponential edge is developed in the drain line. In order to make the velocity of the sinusoidal wave coincident with that of the exponential edge, the wavenumber of this sinusoidal wave must be considerably increased. Moreover, the small-amplitude parts of the wave disappear with the shorter propagation while the large-amplitude ones remain in the drain line. The input pulse is considerably shortened owing to these two properties. This paper validates the pulse-shortening phenomena by performing several measurements using a breadboarded TWFET.

1. INTRODUCTION

It is expected that an incident pulse will experience considerable shortening in a traveling-wave field effect transistor (TWFET) [1]. A TWFET is a special type of FET whose electrodes are employed not only as electrical contacts but also as transmission lines [2]. In this paper, we consider the case in which voltage pulses are simultaneously applied to the gate and drain lines. The typical waveforms are shown in Figure 1. The pulse applied to the drain line must increase, whereas the pulse applied to the gate line must decrease. Moreover, the gate pulse must cross the FET threshold voltage. As far as pulses satisfy these conditions, pulse shortening

Received 20 January 2011, Accepted 22 February 2011, Scheduled 25 February 2011
Corresponding author: Koichi Narahara (narahara@yz.yamagata-u.ac.jp).

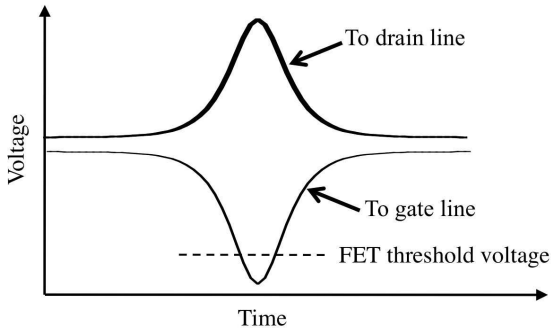

Figure 1. Pulses applied to TWFET.

is guaranteed irrespective of waveform details. When these pulses are applied repeatedly, we can obtain a short electrical-pulse train. By properly designing the top and bottom levels of the applied pulses, each FET simulates an electronic switch that is open for voltages greater than some fixed threshold and closed otherwise. When a pulse crosses the threshold in a transmission line with regularly spaced switches, it is generally observed that a sinusoidal mode supports the pulse at voltages greater than the threshold, while an exponential mode supports the pulse at voltages less than the threshold [3]. For making the velocities of both the modes coincident, the typical wavenumber of the exponential mode must be increased considerably, so that we expect significant shortening of the input pulse. We first briefly review the device configuration and operating principle and then describe the experimental characterizations that validate the theoretical expectations of the pulse-shortening phenomena in TWFETs. Finally, we demonstrate the generation of a short electrical-pulse train from a sinusoidal input.

2. PULSE-SHORTENING PHENOMENA IN TWFETS

Figure 2(a) shows a unit cell of a TWFET. The gate and drain lines are coupled via the gate-to-drain capacitance C_m, the mutual inductance L_m, and the drain-to-source current I_{ds}. The per-unit-cell series inductance and shunt capacitance of the gate (drain) line are denoted by L_g (L_d) and C_g (C_d), respectively.

Because of the presence of electromagnetic couplings between the gate and drain lines, two different propagation modes, called the c mode and the π mode, are developed on a TWFET. Each mode has its own characteristic impedance and velocity [4]. In this paper, we define

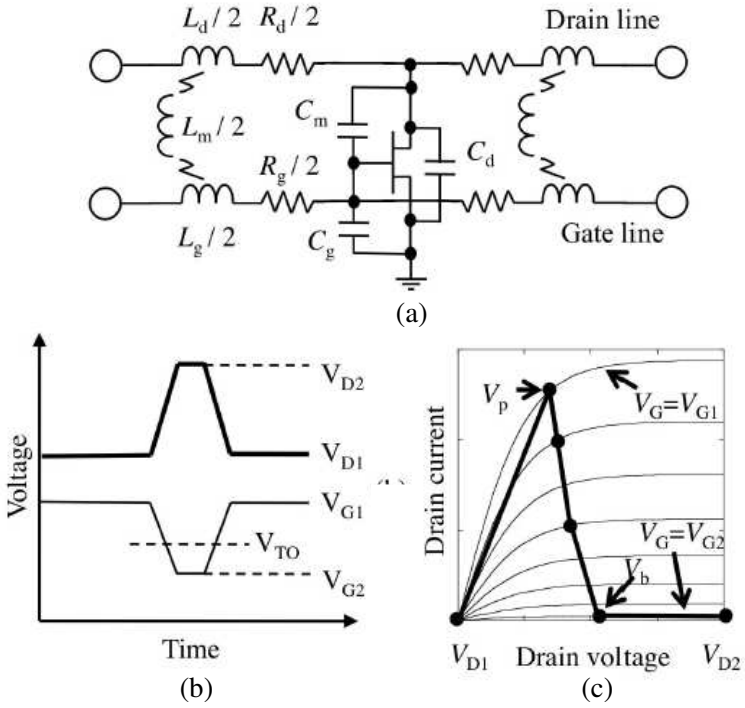

Figure 2. Pulse shortening in TWFETs. (a) Unit cell of a TWFET, (b) signal applications, and (c) effective current voltage relationship on the drain line.

the c mode as being faster than the π mode. We can then design a TWFET to amplify only the pulses carried by one of the two modes and attenuate those carried by the other mode. In particular, a π-mode pulse is uniquely amplified for negligible mutual inductance [5]. Figure 2(b) represents the essential pulse shapes applied at one end of a TWFET required for pulse shortening. The thin and thick pulses correspond to the gate and drain lines, respectively. The voltages biasing the gate and drain lines are denoted as V_{G1} and V_{D1}, respectively. The drain pulse has a parity opposite to that of the gate pulse. Moreover, the top and bottom voltage levels of the drain (gate) pulse are set to V_{D2} (V_{G1}) and V_{D1} (V_{G2}), respectively. At this point, V_{G2} is set below the FET threshold voltage V_{TO}, and both V_{D1} and V_{G1} are set to approximately 0 V. The solid curves in Figure 2(c) show typical drain current voltage relationships for various gate bias voltages. The uppermost and lowermost curves correspond to the relationships for V_{G1} and V_{G2}, respectively. When the pulse is

carried by a unique amplified mode, the leading edges of the gate and drain pulses remain aligned during propagation. Therefore, the drain line effectively exhibits nonlinear conductance shown by the solid curve in Figure 2(c). For convenience, we call the drain voltages less than V_p and greater than V_b regions I and II, respectively. The pulse is influenced by finite shunt conductance in region I and is completely loss-free in region II. Moreover, it is expected that an exponential mode would develop in region I and a sinusoidal mode would develop in region II. For quasisteady pulse propagation, the velocity of the sinusoidal mode in region II must coincide with that of the exponential mode in region I. For this coincidence, the sinusoidal mode must exhibit a large wavenumber. Because the drain line attenuates voltage waves only below V_p, the small-amplitude parts of the wave disappear with the shorter propagation while the large-amplitude parts remain. Finally, a short pulse is obtained at the output. In summary, the input pulse experiences considerable shortening when we design the line to make the wavenumber of the sinusoidal mode in region II as large as possible. For example, the wavenumber tends to become larger for smaller mutual capacitance and larger mutual inductance for a TWFET having the coincident capacitances and inductances, i.e., $C_g = C_d$ and $L_g = L_d$ [1].

3. METHODS AND MATERIALS

We built a 169-section TWFET on a standard breadboard to characterize pulse shortening. The FETs used were TOSHIBA 2SK30A. Inductances and capacitances were implemented using 100 μH inductors (TDK EL0405) and 47 pF capacitors (TDK FK24C0G1), respectively. The test line was fed by a pulse signal generated by a two-channel arbitrary waveform generator NF WF1974. Voltage pulses with the waveform

$$V_{in}\mathrm{sech}^2(\omega_0 t), \tag{1}$$

were input to electrode lines, where ω_0 was set to 0.6 MHz and V_{in} was set to 1.1 and −1.3 V for the drain and gate lines, respectively. Both V_{G1} and V_{D1} were set to zero. The signals along the test line were detected by an Agilent 1134A active probe and monitored in the time domain using an Agilent DSO90254A oscilloscope.

4. RESULTS

Figure 3 shows the measured waveforms monitored at eight different cells on the drain line ($n = 1$, 20, 40, 60, 80, 100, 120, and 140). When

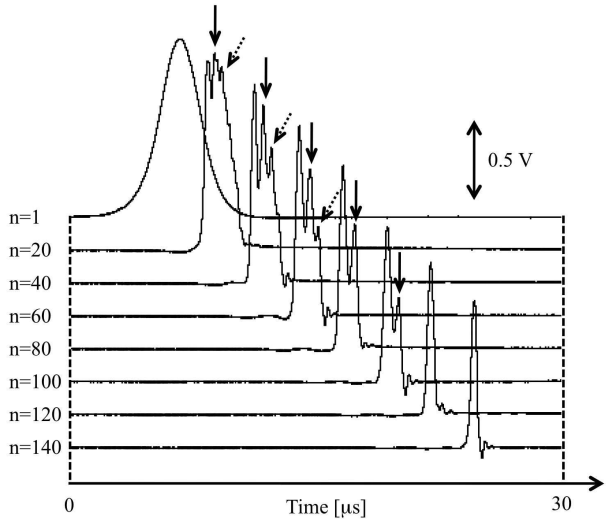

Figure 3. Pulse shortening in a test TWFET. Waveforms monitored at eight different cells are plotted.

the pulse reaches the 20th cell, its leading edge steepens because of the development of the short wavelength exponential mode in region I. After passing the 50th cell, the top of the pulse exhibits oscillation resulting from the development of a short wavelength sinusoidal wave in region II. The second and third peaks of the oscillatory waveforms are emphasized in the figure by solid and dotted arrows, respectively. The third peak decays gradually up to the 60th cell and disappears by the subsequent rapid decay. The second peak survives even when the third one disappears. However, it too disappears at the 120th cell and only the first peak survives, resulting in the development of a short pulse. It was confirmed that the smaller pulses decay more rapidly than the larger ones. Note that the resulting short pulse decays little during propagation from the 120th cell to the 140th cell and the amplitude remains greater than 1.0 V. The full width at half maximum (FWHM) is estimated to be 2.84 and 0.39 μs for the pulses recorded at $n = 1$ and $n = 140$, respectively. The resulting pulse compression ratio, defined by the fraction between the input and output FWHMs, is 7.28.

Using parameters for the test line, the normalized velocities of the test TWFET in regions I and II are shown in Figure 4(a). As previously mentioned, the cross point of velocities in regions I and II determines the width of the shortened pulse. At present, the cross-point frequency f_c and the wavenumber k_c are estimated to be 1.8 MHz and 1.57 rad/cell, respectively. On the other hand, Figure 4(b)

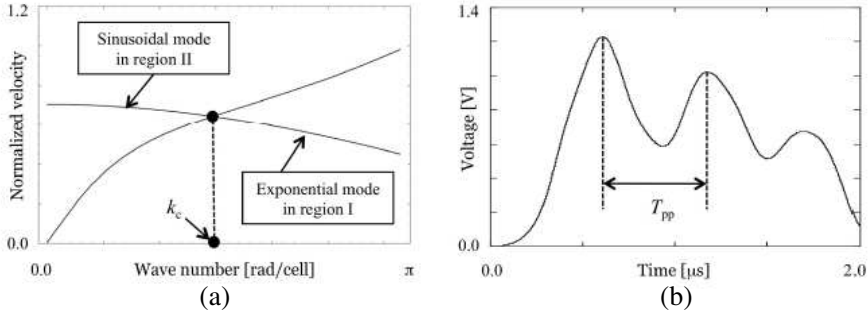

Figure 4. Width of the shortened pulse. (a) Normalized velocities in regions I and II and (b) the frequency of the sinusoidal mode developed in region II.

shows the measured waveform monitored at $n = 50$. The temporal separation between adjacent peaks, T_{pp}, corresponds to the frequency of the sinusoidal mode in region II. The corresponding frequency is estimated to be 1.75 MHz and is well characterized by f_c. To examine the uniqueness of the amplified mode, we show temporal waveforms on both the gate and drain lines of a TWFET monitored at $n = 1$, 50, 100, and 160 in Figure 5. The bold and solid curves in the figure represent the gate and drain waveforms, respectively. As is more clearly observed in the gate than in the drain line, a slow waveform precedes the shortened pulse. We consider these rapid waveforms as the pulses carried by the other mode that did not contribute to pulse shortening. Consequently, the slower π mode pulse is uniquely shortened.

5. DISCUSSION

First, we clarify how the properties of pulses in TWFETs can be simulated by numerical calculations. The FET is represented by the gate-source, gate-drain, and drain-source currents. The gate-source and gate-drain currents are modeled as ordinary diode currents, while the drain-source current is given by the following function of the gate-source voltage, V_{gs}, and the drain-source voltage, V_{ds}:

$$I_{ds}(V_{gs}, V_{ds}) = \beta(V_{gs} - V_{TO})^2 \tanh(2V_{ds}), \tag{2}$$

for $V_{gs} > V_{TO}$, and $I_{ds} = 0$ otherwise, where β and V_{TO} were set to $0.75\,\mathrm{mA/V^2}$ and $-1.8\,\mathrm{V}$, respectively. The parasitic capacitances of an FET are included in $C_{g,d,m}$ and their dependence on the terminal voltages is neglected. The transmission equations of a TWFET are solved using a standard finite-difference time-domain

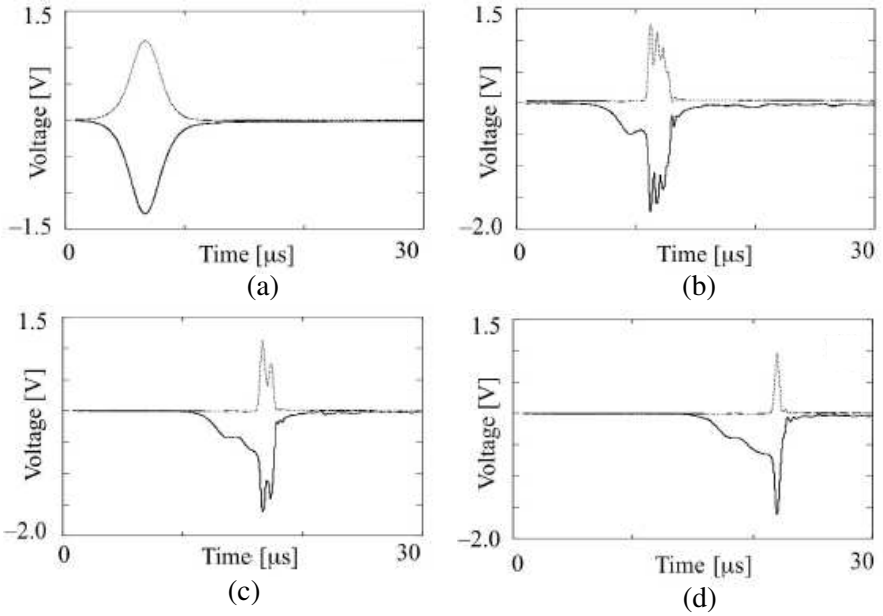

Figure 5. Waveforms on the gate and drain lines. The slow mode contributes to the pulse shortening while the fast mode does not. Temporal waveforms monitored at the 1st, 50th, 100th, and 160th cells are shown in Figures 5(a), (b), (c), and (d), respectively.

method [6]. Figures 6(a) and (b) show the measured and numerically obtained spatial waveforms, respectively, on the drain line recorded in increments of 3.5 μs. As in temporal waveforms, a short-wavelength sinusoidal wave is developed whose smaller peaks decay more rapidly than the largest one. The wavelength of the sinusoidal mode is estimated to be 1.57 rad/cell, which is quite close to k_c. The calculated wavenumber and frequency of the sinusoidal mode are coincident with the measured values. Moreover, the lifetimes of the first, second, and third peaks are correctly described. Although a simple FET model was employed and the variations in device performance were not taken into consideration, the numerical calculations well simulate the measured waveforms.

Finally, we investigate the response of the test TWFET to the sinusoidal signal input. The final width of the shortened pulse is determined by only f_c (or k_c) and does not depend on the input waveform. Therefore, each peak of the drain input evolves into a pulse having the same width as the one obtained in Figure 2. As a result, it is expected that a short-pulse train whose bit rate matches the frequency

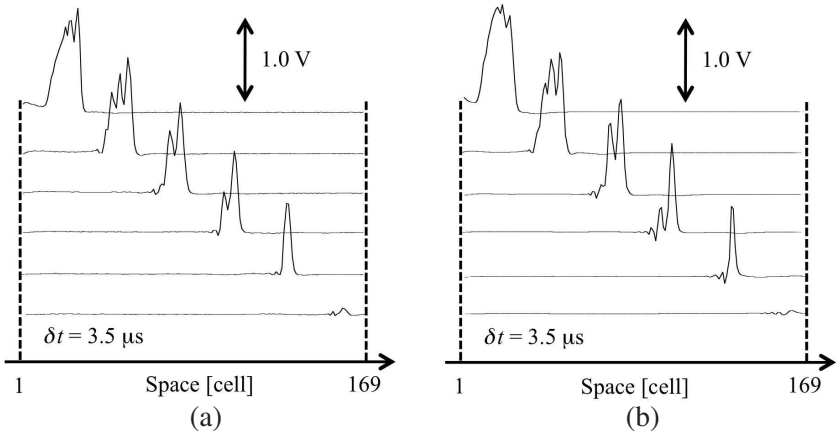

Figure 6. Spatial waveforms on the drain line. (a) Measured and (b) numerically calculated waveforms are shown in increments of 3.5 μs.

of the input sinusoidal signal is output. To examine this expectation, sinusoidal signals with a frequency of 82 kHz and the phase difference set to π are applied at the inputs of the gate and drain lines. The amplitudes of the gate and drain lines are 0.6 and 3.2 V, respectively. In addition, V_{G1} and V_{D1} are set to -0.5 and 1.0 V, respectively. The measured input and output waveforms are shown in Figure 7. Our expectations are successfully confirmed.

As is well known, an electrical nonlinear transmission line (NLTL) [7], which is a transmission line periodically loaded with Schottky varactors, can also operate to generate short electrical pulses. When a step pulse is input into an NLTL such that both nonlinearity and dispersion sharpen the edge, the edge generates a shock [8]. A pulse-reshaping component such as a short stub is required at the end of the line to convert the step pulse into an impulse. This overhead reduces design flexibility in pulse shape and bandwidth. In contrast, when a pulse is input into an NLTL such that varactor nonlinearity compensates for dispersion, the line generates multiple solitonic pulses whose widths are generally smaller than the input width [9]. By extracting the largest pulse, the NLTL operates as a good short-pulse generator. To obtain a shorter pulse, an NLTL must split the input into multiple pulses. Because the separation between split pulses increases only in proportion to propagation length, the number of split pulses is limited by the line length. An NLTL is suitable for generating ultrashort pulses. However, it has several difficulties in design flexibility. In contrast, a TWFET outputs a unique short pulse for any input pulse. In this respect, a TWFET is more advantageous

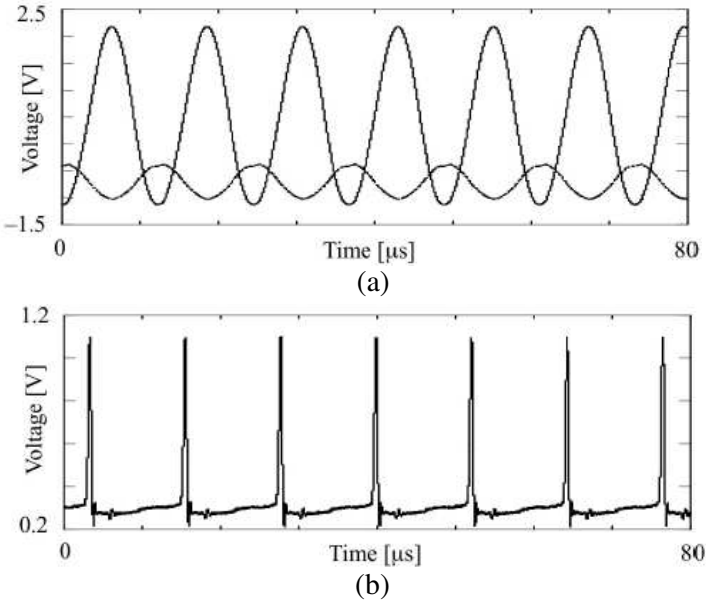

Figure 7. Generation of short-pulse train by sinusoidal signal input. (a) Input and (b) output waveforms. Bold and solid curves represent the drain and gate inputs, respectively, in Figure 7(a). In Figure 7(b), only the drain output is shown.

than an NLTL.

The large-signal FET performance determines how much the pulse width can be reduced. It can be quantified by the maximum operating speed of digital ICs. The relationship between the operation speed of digital ICs and the device figure of merit such as the current-gain cutoff frequency f_T and transconductance g_m has been fully examined [10]. For example, the gate delay becomes 2.0 ps in the rough for an FET with $f_T = 300\,\mathrm{GHz}$ and $g_m = 2.0\,\mathrm{S/mm}$. It is thus expected that the pulse width can be reduced up to several picoseconds for a monolithically integrated TWFET, when implemented with state-of-the-art FET process technologies.

6. CONCLUSION

We investigated pulse shortening in TWFETs using a breadboarded test line. We established that an input pulse experiences pulse shortening because of the development of a short-wavelength sinusoidal wave supported by an exponential wave on the drain line. The

lifetime of the pulse peak and the width of the finally obtained pulses are consistently explained by numerical calculations. Short electrical pulses are engineered in fine-temporal-resolution measurements, wideband communications, and high-resolution imaging systems. By pulse shortening, a TWFET can be utilized as a short-pulse generator. We believe that the device can become the key to achieving breakthroughs in such high-speed systems.

REFERENCES

1. Narahara, K., "Characterization of short pulse generation using traveling-wave field effect transistors," *Jpn. J. Appl. Phys.*, Vol. 50, 014104–014109, 2011.
2. McIver, G. W., "A traveling-wave transistor," *Proc. IEEE*, Vol. 53, 1747–1748, 1965.
3. Narahara, K. and A. Yokota, "Experimental characterization of short-pulse generation using switch lines," *IEICE Electron. Express*, Vol. 5, 973–977, 2008.
4. Gupta, K. C., R. Garg, and I. J. Bahl, *Microstrip Lines and Slotlines*, Artech, 1979.
5. Narahara, K. and S. Nakagawa, "Nonlinear traveling-wave field effect transistors for amplification of short electrical pulses," *IEICE Electron. Express*, Vol. 7, 1188–1194, 2010.
6. Paul, C. R., *Analysis of Multiconductor Transmission Lines*, 252–358, Wiley, New York, 1994.
7. Hirota, R. and K. Suzuki, "Studies on lattice solitons by using electrical networks," *J. Phys. Soc. Jpn.*, Vol. 28, 1366–1367, 1970.
8. Rodwell, M. J. W., S. T. Allen, R. Y. Yu, M. G. Case, U. Bhattacharya, M. Reddy, E. Carman, M. Kamegawa, Y. Konishi, J. Pusl, and R. Pullela, "Active and nonlinear wave propagation devices in ultrafast electronics and optoelectronics," *Proc. IEEE*, Vol. 82, 1037–1059, 1994.
9. Kintis, M., L. Xing, F. Flavia, D. Sawdai, L. K. Kwok, and A. Gutierres, "An MMIC pulse generator using dual nonlinear transmission lines," *IEEE Microwave and Wireless Components Lett.*, Vol. 17, 454–457, 2008.
10. Sano, E. and K. Murata, "An analytical delay expression for source-coupled FET logic (SCFL) inverters," *IEEE Trans. Electron. Devices*, Vol. 42, 785–786, 1995.